NASA TECHNICAL MEMORANDUM

NASA TM 73725

NASA TM 73725

AEROACOUSTIC PERFORMANCE OF A SCOOP INLET

by John M. Abbott
Lewis Research Center
Cleveland, Ohio 44135

TECHNICAL PAPER to be presented at the
Fourth Aeroacoustics Conference
sponsored by the American Institute of Aeronautics and Astronautics
Atlanta, Georgia, October 3-5, 1977

AEROACOUSTIC PERFORMANCE OF A SCOOP INLET

John M. Abbott
National Aeronautics and Space Administration
Lewis Research Center
Cleveland, Ohio

Abstract

Results of a low speed wind tunnel test program are presented which demonstrate the aerodynamic and acoustic performance of a scoop inlet. Engine noise that would normally propagate toward the ground is directed upward by the extended lower lip of the scoop inlet. In addition, more of the scoop airflow comes in from above the inlet than below, leading to relatively higher surface velocities on the upper lip and lower surface velocities on the lower lip. These lower velocities on the lower lip result in a higher attainable angle of attack before internal flow separation occurs.

Introduction

Inlet radiated fan noise has traditionally been reduced using one of two suppression techniques: (1) surface acoustical treatment with or without inlet duct splitters,[1] and (2) sonic or high Mach inlets.[2,3] Both of these methods, however, have certain disadvantages. For example, significant noise reductions with surface acoustical treatment may require considerable increases in inlet length (for more treated area) with corresponding increases in weight, total pressure loss, and ultimately airplane operating cost. Inlet splitters present additional performance losses and are generally disliked by aircraft engine users. The sonic inlet has its main disadvantage in the fact that the complication of variable geometry is required to provide sonic flow in the inlet throat at both takeoff and approach engine flow settings.

A different approach to the problem of inlet noise reduction is to not suppress the inlet radiated noise but to change the directivity of the propagating noise - direct upward the noise that normally would be propagating toward the ground. This redirection technique has been explored extensively in regard to shielding engine rear noise from the ground by use of an over-the-wing engine installation with the upper surface of the aircraft wing serving to direct the rear noise upward.[4] In a similar manner, an inlet with a portion of the lower cowling extended forward, a scoop inlet, can serve to direct upward any noise that would normally propagate out of the front of the engine toward the ground. In the case of a scoop inlet, the noise redirection is due to a combination of an upward reflection from the extended lower lip and also an upward refraction due to the inflow velocity gradients generated within the scoop inlet duct. These mechanisms are illustrated in figure 1 where a comparison is made of the flow fields and forward noise propagation characteristics for a conventional inlet and for the scoop inlet. The scoop inlet tends to draw in more of its airflow from above than below (upper pair of sketches) resulting in velocity gradients within the inlet duct that refract upward forward propagating noise (middle pair of sketches). In addition, the extended lower lip reflects upward noise that would propagate toward the ground with a conventional inlet (lower pair of sketches). The aeroacoustic performance of such a scoop inlet is the subject of the experimental results reported here.

The potential advantage of the scoop inlet over the sonic inlet is obvious - a variable geometry system would not be required provided that the passive scoop inlet would work equally well acoustically at takeoff and approach engine flow settings. Compared with the treated inlet it is hoped that a given amount of noise reduction can be attained with a shorter, lighter, and structurally simpler scoop inlet. The asymmetric shape of the scoop inlet, however, makes the aerodynamic design of the inlet more difficult than for a conventional axisymmetric design. This is particularly true for the cruise condition where the external forebody of the inlet needs to be designed to accommodate an asymmetric flow spillage.

In addition to its potential acoustic benefits, the scoop inlet flow field illustrated in figure 1 suggests a potential for reduced foreign object ingestion into an aircraft engine. When an aircraft is on the ground during takeoff and approach, there would be less of a tendency for sand, rocks, or other particles on the runway to be ingested into an engine with a scoop inlet due to the inlet airflow being drawn in more from above than below. This reduction in foreign object ingestion would lead to longer engine blade life and less of a time degradation in engine blade aerodynamic performance (improved fuel efficiency).

The purpose of the investigation described here was to determine the low speed (takeoff and approach) aerodynamic and directional acoustic performance of a scoop inlet. The 30.48-centimeter diffuser exit diameter scoop inlet was tested in the Lewis Anechoic Wind Tunnel Facility along with a baseline or conventional inlet. Data are presented for free stream velocities of 0, 18 (35 knots) and 41 meters per second (80 knots), angles of attack from 0° to 90° and one-dimensional throat Mach numbers of 0.3, 0.54, 0.63 (design), 0.70, and 0.75. In addition to presenting these experimental results, a discussion of the scoop inlet cruise design problem is included. Analytical predictions of the external flow field at cruise conditions obtained with a two-dimensional potential flow program are presented.

Symbols

a	ellipse semi-major axis of internal lip
b	ellipse semi-minor axis of internal lip
D	diameter
DMAX	inlet total pressure distortion parameter, (maximum total pressure - minimum total pressure)/(average total pressure)
f_f	one-third-octave filter center frequency
f_s	siren blade passage frequency

STAR Category 07

L	length
M_t	one-dimensional throat Mach number
P	total pressure
p	static pressure
V	velocity
α	angle of attack, deg
β	microphone orientation angle, deg
ΔSPL	sound pressure level reduction, (baseline inlet sound pressure level) - (scoop inlet sound pressure level) at same conditions of free stream velocity, angle of attack and throat Mach number
λ_{max}	maximum diffuser wall angle, deg
ψ	inlet circumferential position, deg

Subscripts:

av	average
c	centerbody
d	diffuser
e	diffuser exit
hℓ	highlight
max	maximum
sep	flow separation
t	throat
0	free stream conditions
1	diffuser exit conditions

Apparatus

Installation

The tests were conducted in the Lewis 2.74- by 4.58-meter Anechoic Wind Tunnel Facility.[5] The installation is shown in figure 2. A vacuum system was used in place of a fan or compressor to induce inlet flow. Inlet angle of attack was remotely varied by a turntable on which the test apparatus was mounted. To determine the acoustic properties of the test inlets using the vacuum flow system, a siren was installed in the flow duct downstream of the inlet. The siren was a 13.97-centimeter-diameter single stage fan modified by the addition of struts and a screen just upstream of the rotor to increase its noise level. The siren was located approximately three inlet diameters downstream of the simulator face (fig. 2).

Directional noise measurements were made by use of a microphone located 1.22 meters in front of the inlet face as shown schematically in figure 2. The microphone was remotely rotated about a pivot point at the inlet face allowing noise data to be taken in the flyover plane at various angles relative to the inlet centerline. The anechoic character of the wind tunnel along with more details of the acoustic measurement system are described in references 6 to 8.

Inlet Design

The major variables defining the geometry of the baseline (symmetric) inlet and the scoop inlet are shown in figure 3. Both inlets have a diffuser-exit-diameter, D_e, of 30.48 centimeters with a one-dimensional design throat Mach number of 0.63. The main difference between the two inlets, of course, is that the inlet length, L, is dependent on circumferential location, ψ, for the scoop inlet and constant for the baseline inlet. Note that from circumferential angles of 113.6° to 246.4°, the scoop inlet length is constant and equal to that of the baseline inlet ($L/D_e = 0.716$). As the lower lip of the scoop is approached the length grows, through a lengthening of the inlet throat section, to a maximum value of $L/D_e = 1.295$.

The internal lip design is a 2-to-1 ellipse with a relatively high area contraction ratio, $(D_{h\ell}/D_t)^2$, of 1.44 to prevent internal flow separation at the relatively high angles of attack encountered in a STOL (short takeoff and landing) aircraft application. The external forebody design was selected for a cruise Mach number of 0.76 using design charts for symmetric inlets. This design would be expected to work quite well at cruise with the symmetric baseline inlet. However, the scoop inlet, with its asymmetric spillage properties at cruise, may require a different external forebody design.

Instrumentation and Data Reduction

Aerodynamic

Inlet aerodynamic performance was evaluated through use of static pressure taps on the inlet surfaces and total pressure rakes located at the inlet diffuser exit. A total of 85 internal surface static pressure measurements were made with the scoop inlet and 69 with the baseline inlet. Diffuser exit total pressure measurements were made using both hub and tip boundary layer rakes as well as rakes spanning the entire annulus. Eight full-span total pressure rakes (equally spaced circumferentially) were used with six equal-area-weighted tubes per rake. The 16 boundary layer rakes (eight at the hub and eight at the tip) each contained five total pressure tubes.

Inlet total pressure recovery, $P_{1,av}/P_0$, was computed using all measured total pressures, including boundary layer rakes, with the appropriate area weighting terms. However, in computing inlet total pressure distortion, DMAX, boundary layer measurements taken closer to the wall than the nearest tube on the six element equal-area-weighted rakes were omitted. Inlet one-dimensional throat Mach number, M_t, was computed using the inlet weight flow measured by a venturi located downstream in the flow duct and the geometric throat area assuming uniform flow.

Acoustic Data

Directional noise measurements were made by use of a microphone located 1.22 meters in front of the inlet face. The microphone was remotely

rotated about a pivot point at the inlet face allowing noise data to be taken in the flyover plane at various angles relative to the inlet centerline. An online graphic display of noise levels provided a continuous trace of one-third-octave sound pressure level versus microphone orientation angle, β, as the microphone rotated. Any one-third-octave band could be selected for the trace. In addition, the microphone was positioned at fixed values of β where magnetic tape data were recorded for later one-third-octave spectral analysis. A complete description of the noise data acquisition system in the Lewis Anechoic Wind Tunnel can be found in reference 8.

Procedure

Aerodynamic and acoustic testing were done separately. During the aerodynamic tests, the noise siren was not used. During the acoustic tests, the inlet weight flow was set at the desired value, the siren speed was adjusted to set the blade passing frequency at the desired value and the acoustic data were taken.

Results and Discussion

Aerodynamic Performance

The basic aerodynamic performance of the scoop and baseline inlets is shown in figure 4 in terms of total pressure recovery and distortion versus throat Mach number. In figure 4(a), static performance is shown and indicates lower recoveries and higher distortions for the scoop inlet as compared to the baseline inlet over the entire range of throat Mach number. At the design throat Mach number of 0.63, the recovery and distortion are 0.985 and 0.15 for the scoop inlet and 0.993 and 0.025 for the baseline inlet. The reason for the lower level of aerodynamic performance for the scoop inlet will become apparent in a later discussion of the inlet surface static pressure distributions.

At a free stream velocity of 41 meters per second and 0° angle of attack (fig. 4(b)), the aerodynamic performance of the scoop inlet has improved considerably over that at static conditions although it is still slightly lower than the baseline inlet. For example, at a throat Mach number of 0.63, the recovery and distortion are 0.992 and 0.045 for the scoop inlet and 0.994 and 0.006 for the baseline inlet. Reasons for this improved performance will again become apparent in a later more detailed discussion.

Figure 4(b) also shows inlet performance at an angle of attack of 50°. (An angle of attack considered to be the maximum value encountered by an inlet in a STOL aircraft installation.) The relative ranking of the inlets remains the same. At the design throat Mach number of 0.63, the scoop inlet recovery is 0.989 and the distortion is 0.15. The values for the baseline inlet are 0.993 and 0.04, respectively.

The circumferential variations of surface static pressure at the inlet highlight for both the scoop and baseline inlets are shown in figure 5. At static conditions (fig. 5(a)), the relatively flat distribution of static pressure for the baseline inlet indicates the inflows to this inlet is circumferentially uniform. The static pressure distribution for the scoop inlet, however, indicates low highlight static pressure (high surface velocities) over the upper half of the inlet ($\psi > 90^\circ$) and high static pressures (low surface velocities) over the lower half of the inlet ($\psi > 90^\circ$). This distribution is a result of more of the scoop inlet airflow coming in from above than below. The high surface velocities over the upper portion of the scoop inlet account for the lower recovery and higher distortion of the scoop at static conditions. A detailed examination of the distribution of total pressure at the inlet diffuser exit confirmed that the scoop total pressure losses at static conditions occurred in the upper half of the inlet duct near the outer wall.

At a free stream velocity of 41 meters per second and an angle of attack of 0° (fig. 5(b)), the circumferential distribution of highlight static pressure for the baseline inlet remains flat indicating the inlet inflow remains circumferentially uniform. For the scoop inlet the circumferential distribution of highlight static pressure has the same character as it did at static conditions, however, the total amount of variation is not as great. The introduction of free stream velocity has led to lower surface velocities on the upper portion of the inlet and just slightly higher surface velocities on the lower portion indicating a more circumferentially uniform inflow than at static conditions. This reduction in surface velocity over the upper portion of the scoop accounts for the improved levels of recovery and distortion with forward velocity shown in figure 4(b).

Increasing angle of attack to 50° (fig. 5(c)), results in a large decrease in surface static pressure (increase in surface velocity) on the lower lip ($\psi = 0^\circ$) of the baseline inlet while the lower lip of the scoop inlet has very modest surface velocities. It appears that the $\psi = 100^\circ$ position (near the "corner" in the side profile) is the more critical region in terms of high surface velocities with the scoop inlet as angle of attack is increased. A detailed examination of the distribution of total pressure at the diffuser exit indicates that the total pressure losses encountered with the scoop at an angle of attack of 50° are concentrated near the $\psi = 110^\circ$ circumferential position. The nature of the distribution also suggests that the indicated low values of total pressure may be the result of vortices being formed in the "corners" of the scoop side profile and propagating back to the diffuser exit. It is possible that a modification of the side contour (to decrease the sharpness of the "corner") may eliminate or reduce the strength of these vortices and improve the inlet aerodynamic performance accordingly.

At angle of attack, the lower surface velocities on the lower lip of the scoop inlet compared to the baseline inlet result in a higher attainable angle of attack for the scoop before inlet flow separation is encountered. This is illustrated in figure 6 where the angle of attack where flow separation occurred is plotted versus throat Mach number for both inlets at a free stream velocity of 41 meters per second. Below the curves the flow is attached and above it is separated. The data indicate that the separation bound for the scoop inlet is from 7° to 15° higher than the baseline inlet over the range in throat Mach number. At the design throat Mach number of 0.63, the flow separation

angle for the baseline inlet is 71° and for the scoop inlet is 84°.

To reiterate, the higher flow separation angles attainable with the scoop inlet are a result of the natural tendency of the incoming flow to be drawn in from above, thus reducing the surface velocities on the critical lower lip. And again, the critical region with this particular scoop inlet may be the side "corner" which if made less severe, could result in even higher flow separation angles.

The diffuser exit total pressure contours for the scoop inlet in a 90°, 18-meter-per-second (35-knot) crosswind is shown in figure 7 at the design throat Mach number of 0.63. The results are similar over the full throat Mach number range. The figure indicates a poor level of performance of the scoop in a 90° crosswind. The initial suspicion might be that the flow has separated from the side of the inlet. However, an examination of the axial distribution of surface static pressure at circumferential positions of 0°, 45°, 60°, 90°, and 100°, does not indicate the presence of any flow separation. It is likely that a vortex has formed in the "corner" of the side profile which is resulting in the indicated low total pressures due to excessive flow angularity into the total pressure probes. A modified side contour may eliminate or reduce the strength of this vortex.

Acoustic Performance

Shown in figure 8 are typical on-line directional noise traces obtained by rotating the microphone through an orientation angle, β, from -110° to +110°. (Negative angles are below the inlets, positive angles above.) Traces are shown for the scoop and baseline inlets at a free stream velocity of 41 meters per second at an angle of attack of 0° and at the design throat Mach number of 0.63. The siren speed was adjusted so that the blade passing frequency was at 9600 Hz. The acoustic traces for the two inlets represent the sound pressure level in the 8000-Hz center frequency one-third-octave band. A third trace, at the same frequency, is shown in the figure and represents the background level in the anechoic wind tunnel obtained at a free stream velocity of 41 meters per second with the siren turned off and no flow through the inlet.

A comparison of the noise levels for the baseline inlet and the scoop inlet in figure 8 indicates that the scoop inlet is providing a reduction in the noise that would normally propagate toward the ground (negative values of β). The amount of noise reduction relative to the baseline inlet, designated as ΔSPL in the figure, is a maximum of about 15 dB at a microphone orientation angle of -80° and still about 5 dB along the inlet centerline (β = 0°). Even for positive values of β (above the inlet) the sound pressure level of the scoop inlet is lower than that of the baseline. This somewhat surprising effect at positive β is probably the result of high flow Mach number suppression in the upper portion of the inlet duct due to the incoming flow asymmetry. (Refer to the discussion of fig. 5.) A detailed discussion of the high Mach number suppression principle can be found in reference 3.

Traces like those shown in figure 8 were also taken in the 10 000 Hz one-third-octave band containing the siren blade passing tone. The conclusions that were made regarding the 8000 Hz data also apply to the 10 000 Hz data. The traces taken in the 10 000 Hz one-third-octave band, however, generally had a wider variation in sound pressure level at a given microphone orientation angle than the 8000 Hz data, suggesting a time unsteadiness in the siren blade passing tone.

Figure 9 shows the entire one-third-octave spectra for the scoop inlet, baseline inlet and background noise at a fixed microphone orientation of -60°. All the test conditions are identical to those in figure 8. The spectra indicate that the scoop inlet is providing a substantial level of noise reduction, ΔSPL, over the range of frequency where the background noise level is not an interfering factor (greater than about 2000 Hz). Noise reduction values range from 8 dB at 2000 Hz to 12.5 dB at 20 000 Hz.

Figure 10 shows the effect of inlet throat Mach number on the noise reduction, ΔSPL, of the scoop inlet as a function of microphone orientation angle at a free stream velocity of 41 meters per second and an angle of attack of 0°. The value of ΔSPL at each microphone orientation angle was obtained by subtracting the noise level of the scoop inlet from that of the baseline inlet with both inlets operating at the exact same conditions of free stream velocity, throat Mach number, angle of attack and siren speed. The data indicate that over the range in throat Mach number from 0.31 to 0.70, the scoop inlet effectively provides noise reduction below the inlet with maximum noise reductions on the order of 15 dB. No systematic effect of throat Mach number is apparent below the inlet (negative β), however, there is a systematic increase in noise reduction above the inlet with increasing Mach number. This again is a result of the progressive effect of increasing high Mach number suppression occurring in the upper portion of the scoop inlet due to the flow asymmetry in the inlet duct.

The effect of angle of attack on the noise reduction directivity of the scoop inlet is shown in figure 11 for angles of attack of 0°, 15°, and 30° at a free stream velocity of 41 meters per second and the design throat Mach number of 0.63. The data for angles of attack of 0° and 15° are very nearly the same. At a 30° angle of attack, there appears to be a slight decrease in the amount of noise reduction provided by the scoop inlet over the full range of microphone orientation angle. However, it is at most a 4-dB loss in noise reduction, relative to the 0° angle of attack data at a microphone orientation angle of -90°, and more typically on the order of 1 to 2 dB over most of the range of microphone orientation angle.

Cruise Performance

The inlet external flow fields at cruise for both the baseline and scoop inlets are shown in figure 12 at a free stream Mach number of 0.75, the design throat Mach number of 0.63 and an angle of attack of 0°. The results were obtained from a two-dimensional, incompressible potential flow analysis using the method of reference 9. The figure indicates the size and location of the capture streamtube - the streamtube of air that actually goes in the inlet. Also shown is the size and location of the spillage airflow - that airflow which

must eventually pass around the inlet. Note that for the baseline inlet (fig. 12(a)), the capture streamtube is symmetric about the inlet centerline and equal amounts of air must be spilled over the upper and lower external forebody. An external forebody shaped to efficiently turn the spillage flow around the inlet for this type of flowfield would be designed using design charts like those reported in reference 10. With the scoop inlet, however, the capture streamtube is not centered on the inlet centerline but is displaced downward toward the lower lip. This results from the difference in length between the upper and lower lips. The free stream flow is not aware of the presence of the upper lip as soon as the lower lip, hence less flow is spilled over the lower lip than would normally spill for a symmetric inlet, leaving more flow to be spilled over the upper lip. In particular for this case, 40 percent of the spillage flow is over the lower lip and 60 percent over the upper lip. Hence, the geometric design of the external forebody for a scoop inlet may have to vary circumferentially in order to maintain attached, shock-free flow around the inlet. In this case, use may still be made of the external forebody design charts developed for symmetric inlets, with some change in interpretation.

Summary of Results

Wind tunnel tests were conducted to determine the aerodynamic and acoustic performance of a scoop inlet. Compared with an axisymmetric baseline inlet, the scoop inlet generated higher velocities in the vicinity of the upper lip and lower velocities about the lower lip. This accounts for most of the following results.

1. At static conditions the recovery was lower and distortion higher for the scoop inlet when compared with the baseline inlet. This resulted from higher total pressure losses in the upper portion of the scoop inlet duct due to the high upper lip surface velocities. Free stream velocity improved the scoop inlet performance considerably bringing it nearly to the level of the baseline inlet.

2. Increasing angle of attack to 50° at a free stream velocity of 41 meters per second resulted in higher total pressure losses for the scoop inlet with the losses being concentrated downstream of the "corners" in the scoop side profile. These indicated total pressure losses may be a result of vortices being formed in the "corners" and propagating back to the diffuser exit. These same results were apparent with an 18-meter-per-second, 90°-crosswind. An appropriate modification to reduce the severeness of the "corner" may eliminate the problem.

3. At a given angle of attack, the relatively lower surface velocities on the lower lip of the scoop inlet (when compared to the baseline inlet) resulted in a higher attainable angle of attack before the internal flow separated. For example, at a free stream velocity of 41 meters per second, the flow separation angles for the scoop inlet were as much as 15° higher than those for the baseline inlet over the range of throat Mach number.

4. Acoustically, the scoop inlet provided a maximum noise reduction of from 12 to 15 dB below the inlet over the entire range of throat Mach number and angle of attack at a free stream velocity of 41 meters per second. The noise reduction occurred from 2000 to 20 000 Hz.

5. Results of a two-dimensional, incompressible potential flow analysis indicated that at cruise, the flow spillage about the scoop inlet is asymmetric with more flow being spilled over the upper lip than the lower lip. This may make the aerodynamic design of the inlet external forebody for efficient cruise more difficult than for a conventional axisymmetric design.

References

1. "Aircraft Engine Noise Reduction," NASA SP-311, 1972.

2. Abbott, J. M., "Aeroacoustic Performance of Scale Model Sonic Inlets," AIAA Paper 75-202, Pasadena, Calif., 1975.

3. Miller, B. A., "Experimentally Determined Aeroacoustic Performance and Control of Several Sonic Inlets," AIAA Paper 75-1184, Anaheim, Calif., 1975.

4. "Aeronautical Propulsion," NASA SP-381, 1975.

5. Yuska, J. A., Diedrich, J. H., and Clough, N., "Lewis 9- by 15-Foot V/STOL Wind Tunnel," NASA TM X-2305, 1971.

6. Rentz, P. E., "Softwall Acoustical Characteristics and Measurement Capabilities of the NASA Lewis 9x15 Foot Low Speed Wind Tunnel," Bolt Beranek and Newman, Inc., Canoga Park, Calif., Rept. BBN-3176, 1976; also NASA CR-135026.

7. Diedrich, J. H. and Luidens, R. M., "Measurement of Model Propulsion System Noise in a Low-Speed Wind Tunnel," AIAA Paper 76-91, Washington, D.C., 1976.

8. Dietrich, D. A., Heidmann, M. F., and Abbott, J. M., "Acoustic Signatures of a Model Fan in the NASA-Lewis Anechoic Wind Tunnel," AIAA Paper 77-59, Los Angeles, Calif., 1977.

9. Hess, J. L. and Smith, A. M. O., "Calculation of Potential Flow About Arbitrary Bodies," in Progress in Aeronautical Sciences, Vol. 8, D. Kuchemann, ed., Pergamon Press, 1967, pp. 1-138.

10. Hancock, J. P. and Hinson, B. L.,"Inlet Development for the L-500," AIAA Paper 69-448, Colorado Springs, Colo., 1969.

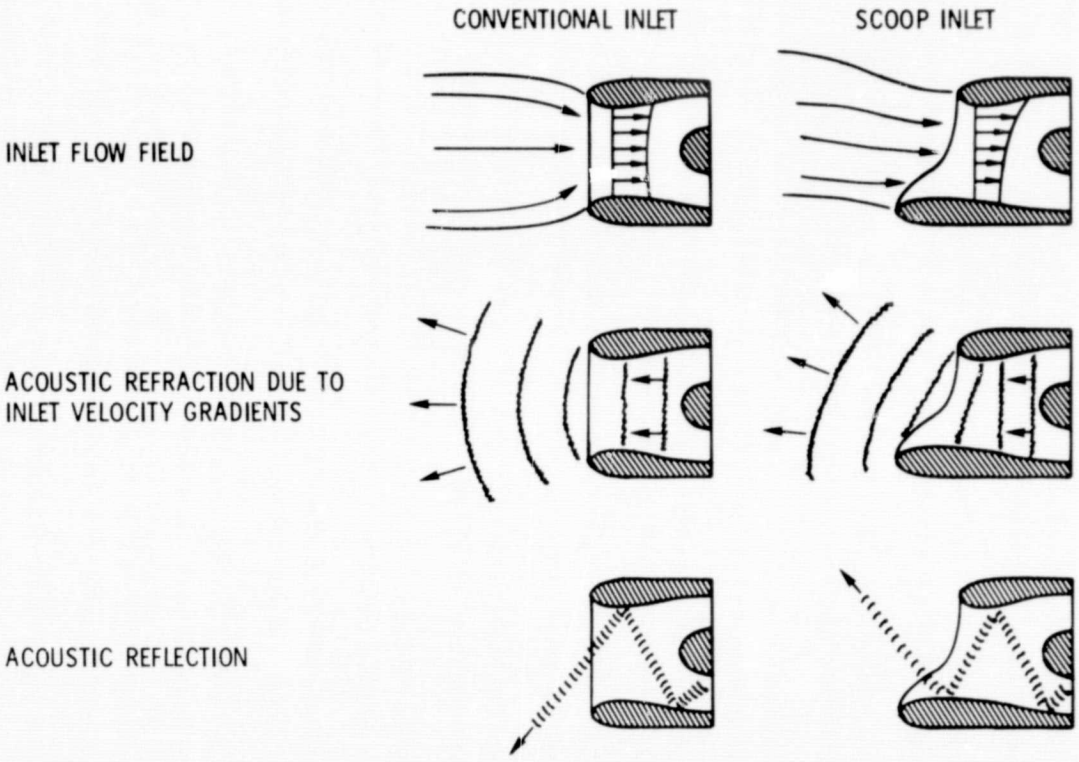

Figure 1. - Inlet flow fields and acoustics.

E-9277

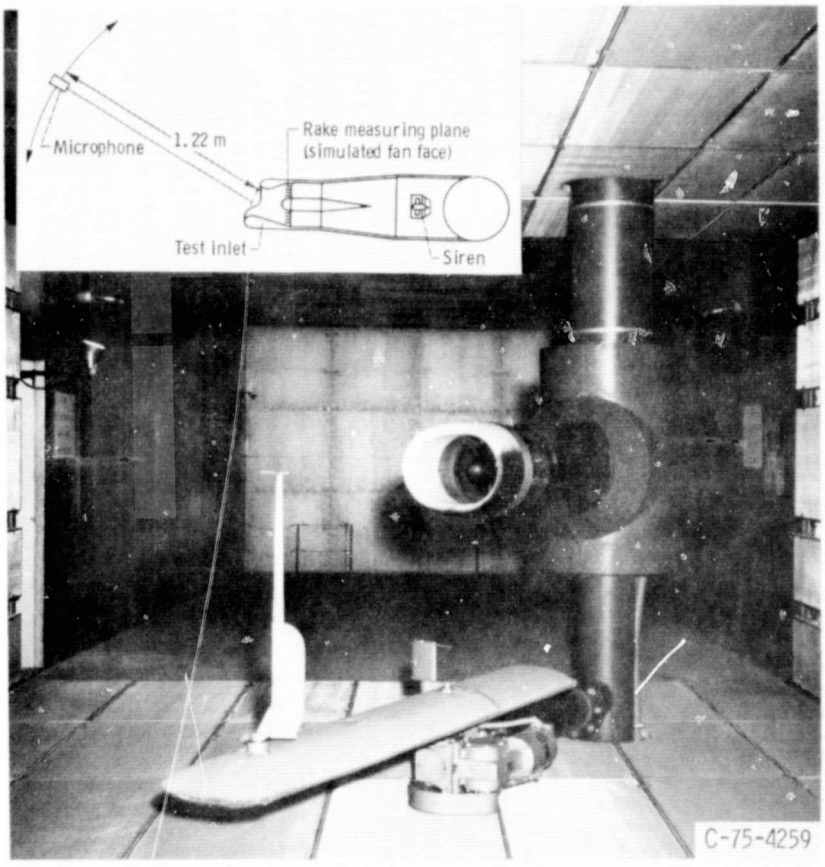

Figure 2. - Test installation in 2.74- by 4.58-meter (9- by 15-ft) anechoic wind tunnel.

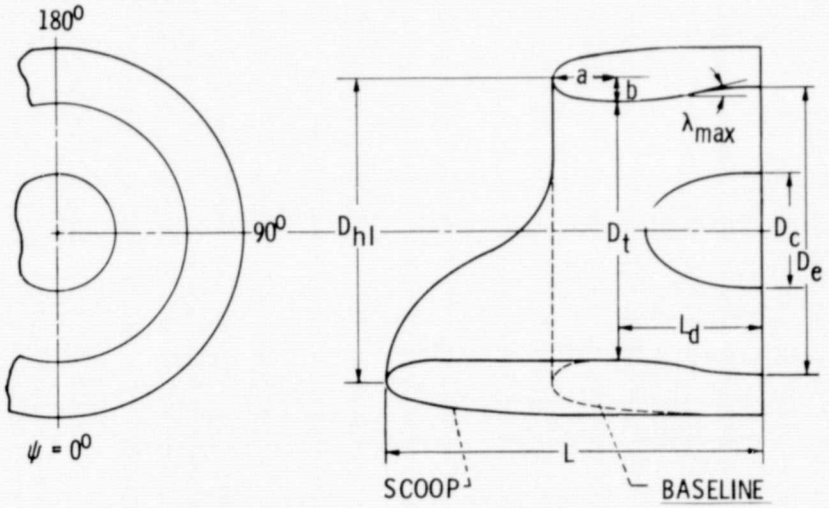

LIP	$(D_{hl}/D_t)^2$	1.44
	a/b	2.0
DIFFUSER	$(D_e - D_c)^2/D_t^2$	1.048
	L_d/D_e	0.538
	λ_{max}	8.37°

DESIGN PARAMETERS; SCOOP AND BASELINE INLETS.

ψ, deg	L/D_e
0	1.295
30 330	1.290
45 315	1.266
60 300	1.207
90 270	0.823
100 260	0.746
105 255	0.727
113.6 ↓ 296.4	0.716

CIRCUMFERENTIAL VARIATION OF LENGTH FOR SCOOP INLET

Figure 3. - Inlet design.

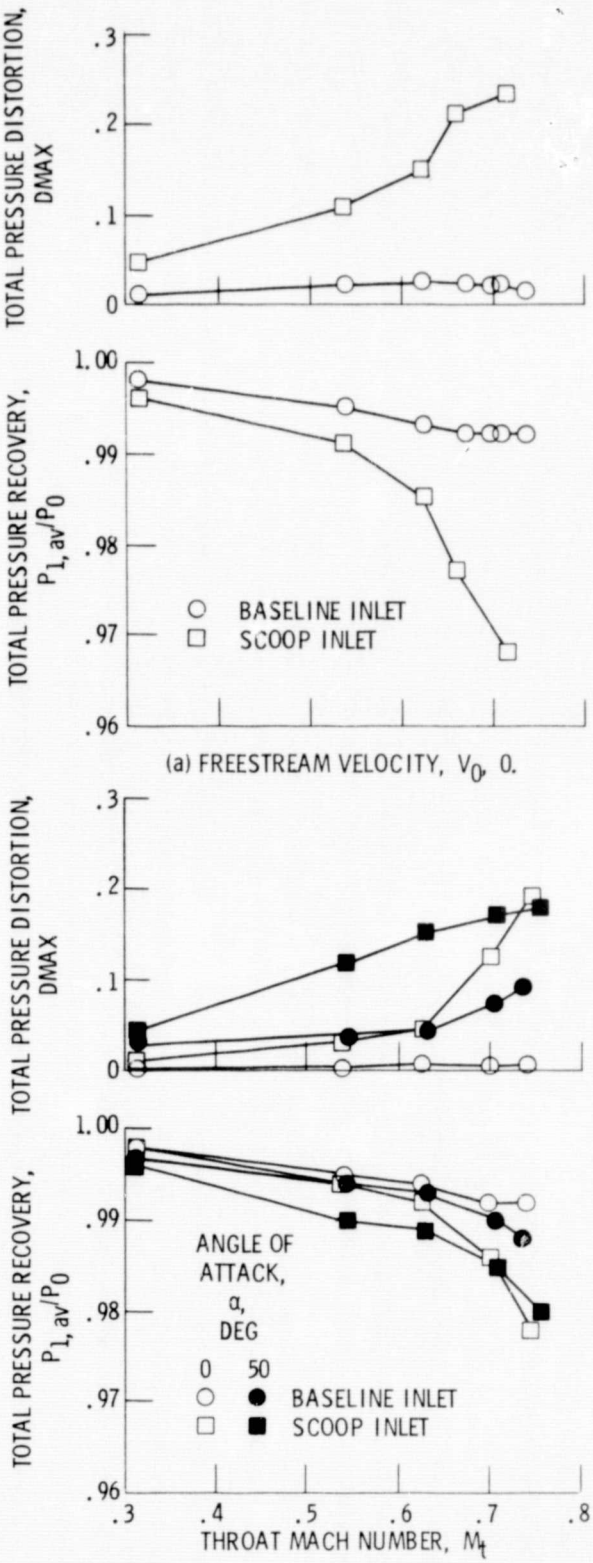

Figure 4. - Aerodynamic performance of scoop and baseline inlets.

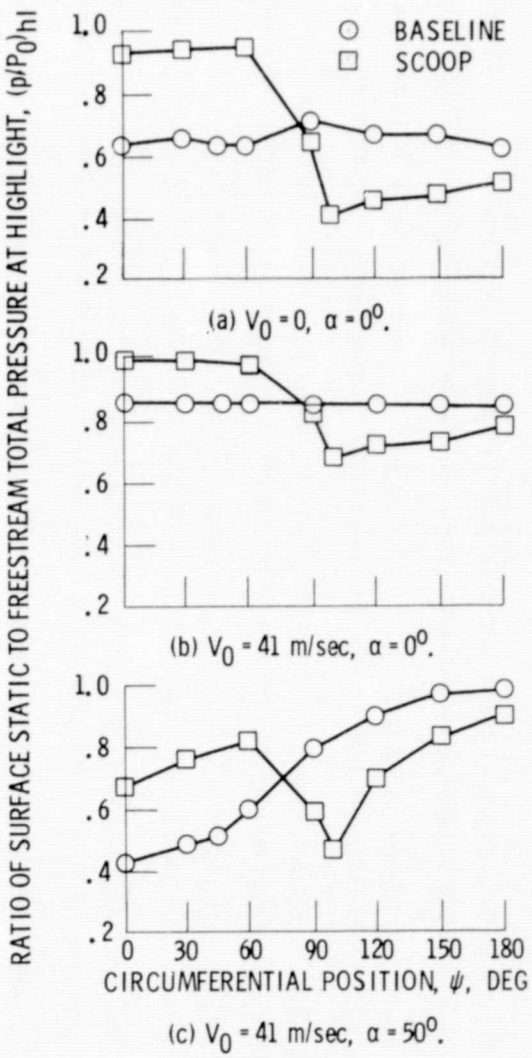

Figure 5. - Circumferential variation of surface static pressure at highlight. $M_t = 0.63$ (design).

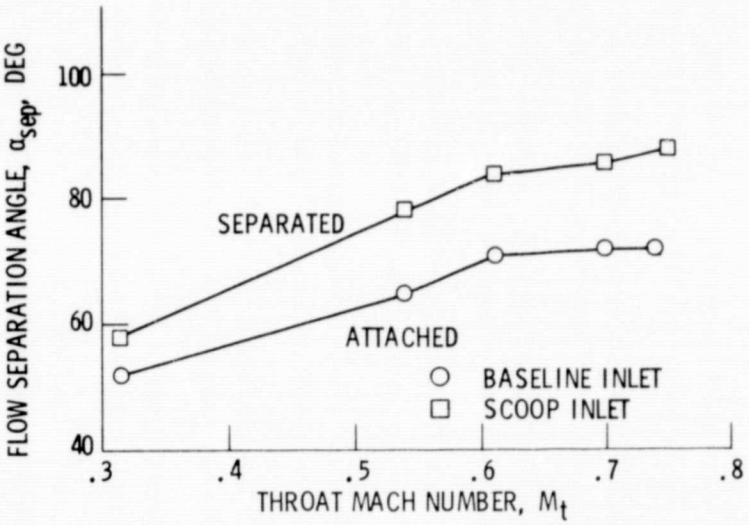

Figure 6. - Flow separation bounds for scoop and baseline inlets. V_0, 41 m/sec.

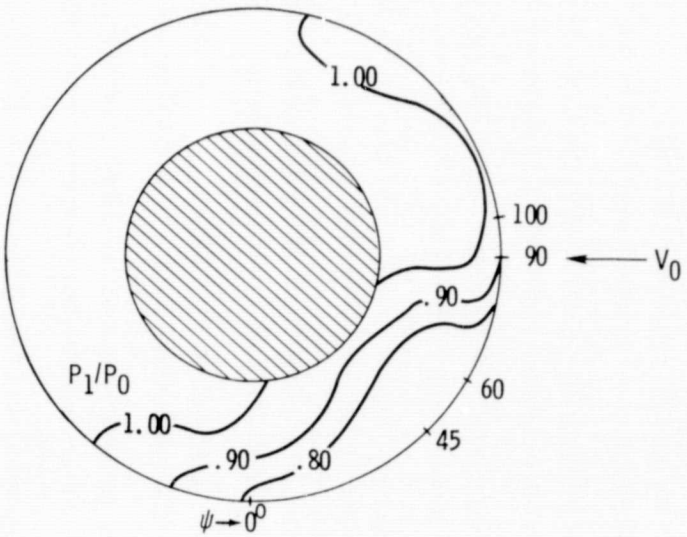

Figure 7. - Distribution of total pressure at diffuser exit for scoop inlet in 90^0 crosswind. V_0, 18 m/sec; M_t, 0.63.

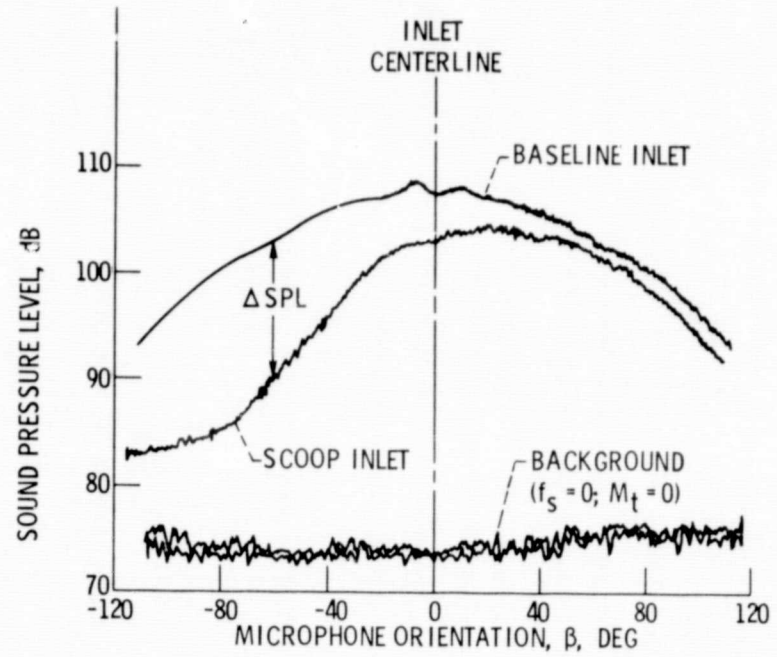

Figure 8. - Comparison of noise directivity for scoop and baseline inlets. V_0, 41 m/sec; α, 0^0; M_t, 0.63; f_s, 9600 Hz; f_f, 8000 Hz.

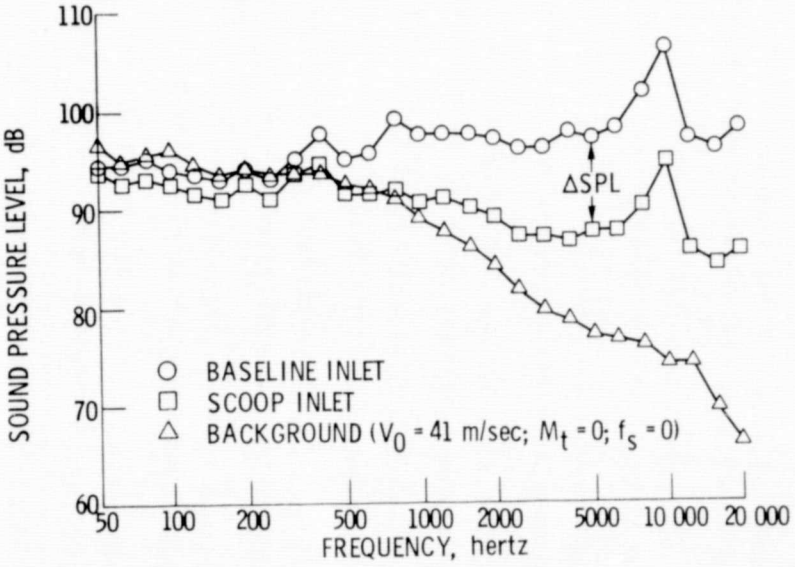

Figure 9. - Comparison of 1/3-octave spectra for scoop and baseline inlets. V_0, 41 m/sec; α, 0^0; M_t, 0.63; f_s, 9600 Hz; β, -60^0.

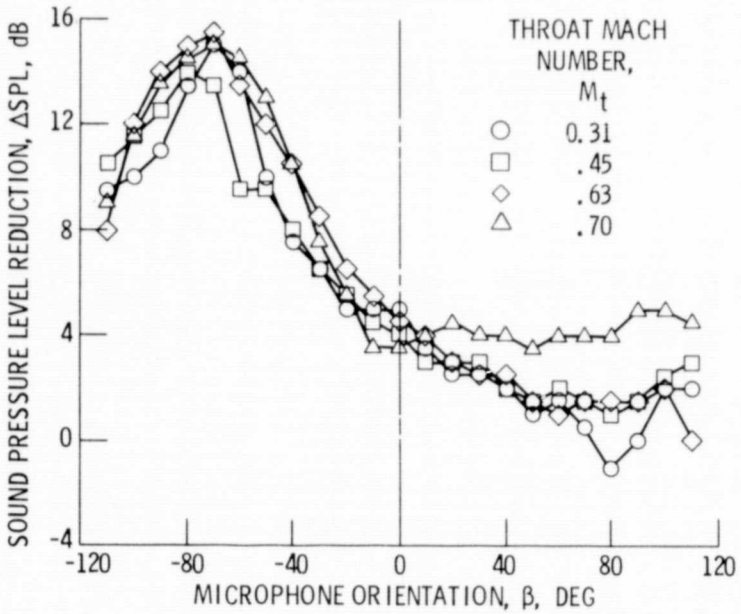

Figure 10. - Effect of throat Mach number on scoop inlet noise reduction. V_0, 41 m/sec; α, 0^0; f_s, 9600 Hz; f_f, 8000 Hz.

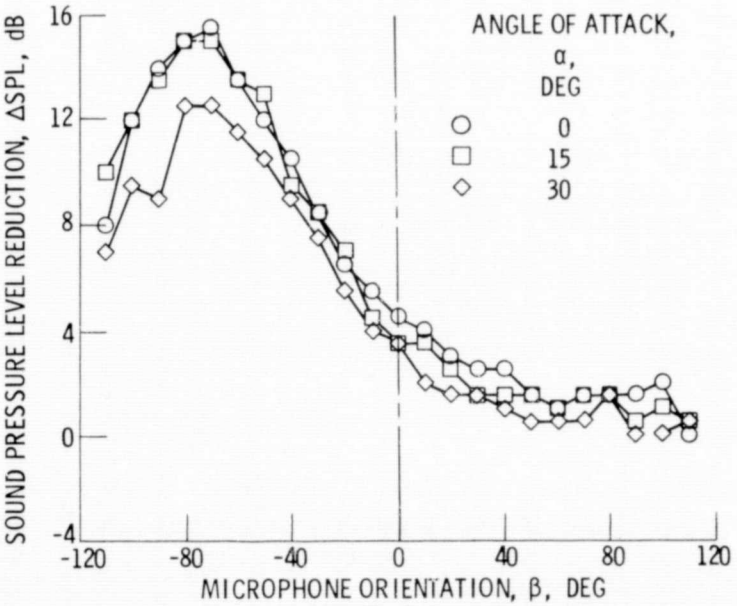

Figure 11. - Effect of angle of attack on scoop inlet noise reduction. V_0, 41 m/sec; M_t, 0.63 (design); f_s, 9600 Hz; f_f, 8000 Hz.

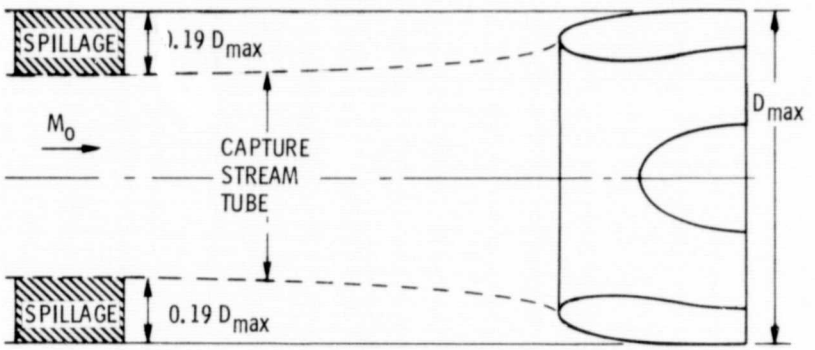

(a) BASELINE INLET.

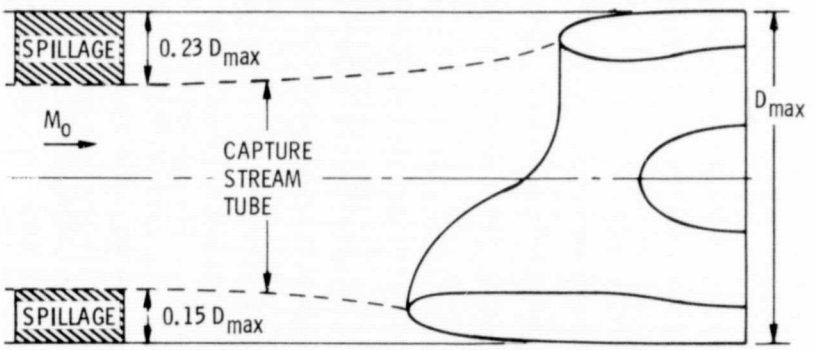

(b) SCOOP INLET

Figure 12. - Scoop and baseline inlet flow fields at cruise. M_0, 0.75; of 0 deg; M_t, 0.63 (design). Two-dimensional, incompressible potential flow analysis.